The preparation of Al_2O_3/M (Fe, Co, Ni) nanocomposites by mechanical alloying and the catalytic growth of carbon nanotubes

J. Ding[a,*], B. H. Liu[a], Z. L. Dong[b], Z. Y. Zhong[c], J .Y. Lin[c], T. White[b]

[a]Department of Materials Science, Faculty of Science, National University of Singapore, Lower Kent Ridge Road, Singapore 119260 Singapore
[b]Environmental Technological Institute of Singapore, Singapore 637723, Singapore
[c]Department of Physics, Faculty of Science, National University of Singapore, Singapore 119260, Singapore
** Corresponding author. Tel.: +65-874-4317; fax: +65-776-3604. E-mail address: masdingj@nus.edu.sg (J. Ding).*

ABSTRACT

Mechanical alloying was employed to produce Al_2O_3/M (M=Fe, Co, Ni) nanocomposites. It was found that high-energy mechanical milling could realize not only drastic refinement but also the well dispersion of catalyst precursors in oxide matrixes. After mechanical milling, the solid-state alloying and the accelerated substitutional reactions were observed between the parent oxides. The as-obtained Al_2O_3/M nanocomposites possessed the fine-grained and porous structures and thus high reducibility. Large-scale formation of multiwalled and single-walled carbon nanotubes were achieved by using these mechanical alloying-derived Al_2O_3/M nanocomposites.

1. INTRODUCITON

Carbon nanotubes (CNTs) are promising nanostructured materials due to their extraordinary mechanical, electric and thermal prosperities. Their light, strong and high toughness characteristics endow them the promising potentials of the applications on the advanced nanocomposites, such as nanotubes/polymer composites [1].

For the catalytic growth of CNTs, one of the key processes is to get sufficiently small metallic particles, which are active enough for the catalytic decomposition of carbon-containing gas [2]. To avoid the rapid coarsening of metallic nanoparticles at high temperature during reduction and carbonization reactions, substrates (usually oxides) always plays crucially important roles. In this sense, the uniform dispersion of catalyst precursors (transition metal oxides) in the substrates is definitely the first important step. Currently, the methods for the precursor preparation were usually based on the wet-chemistry processes, such as sol– gel [3], co-precipitation [4] and impregnation processes [5] as well as the formation of the solid solution between the parent oxides [6]. These methods have been widely employed to produce suitable catalyst for the growth of either

single-walled CNTs (SWCNTs) or multi-walled CNTs (MWCNTs). However, the precursors obtained by these methods are generally required to be thermally treated at certain temperature in order to get desirable phase compositions, for instance, the decomposition of nitrates into oxides [3–6]. This leads to the formation of large-sized agglomerates and thus a large amount of catalyst precursors are trapped inside the agglomerates, which will definitely decrease the productivity of CNTs.

As it is well known, mechanical milling is a powerful tool for producing nanosized powders and nanocomposite materials [7–10]. In addition, high-energy mechanical milling can often accomplish the solid-state alloying, mechanical alloying. Such kinds of mechanical activation effects permit the formation of equilibrium or non-equilibrium phases directly without any thermal treatments or with low-temperature annealing [11–15]. In this work, mechanical alloying process was employed for the preparation of Al_2O_3/M (M=Fe, Co, Ni) nanocomposites on which MWCNTs and SWCNTs were produced with high yields. The effects of mechanical alloying on the morphologies and phase compositions of catalyst precursors and thereby the morphologies and productivity of as-grown CNTs were studied.

2. EXPERIMENTS

A mixture of transition metal (nickel, cobalt and iron) hydroxides powders and Al_2O_3 powder was mechanically milled for 24 h using Spex 8000 high-energy shaker mill. The mass ratio of Al_2O_3 to metal hydroxides was fixed, corresponding to 20 wt% transition metal oxides. For studying the effects of catalyst-loading, another batch of Al_2O_3/FeO_xH_y sample was also prepared by mechanical milling with the mass content of Fe_2O_3 equal to 5 wt%. In order to study the reduction behaviors of different samples, hydrogen reduction were conducted at different temperatures for 40 min. The growth of CNTs was conducted in methane gas at the temperatures between 600 and 1000 ℃ for 40 min.

For the mechanical-alloying derived samples before and after hydrogen reduction, their phase compositions were examined by X-ray diffraction (Philips PW 1820 diffractometer with Cu K_α radiation). In order to monitor the reduction of different samples, magnetic measurements (superconducting vibrating sample magnetometer (VSM), Oxford instruments) were carried out at room temperatures. The saturation magnetization (M_s) was measured at the maximum magnetic field of 30 kOe. In addition, for Al– Fe–O nanocomposites, room-temperature ^{57}Fe Mössbauer spectrometer was used for the analysis of the phase changes induced by mechanical alloying and hydrogen reduction. The morphologies of nanocomposites before and after hydrogen reduction were studied by transmission electron microscope (TEM, JEM-100CX) and Filed-emission Scanning Electronic Microscopy (FE-SEM, Philips, XL30FEG). SEM, low-resolution TEM and High-resolution transmission electronic microscopy (HRTEM, JEL-300CX) were used for the study of the morphologies of carbon products.

3. RESULTS AND DISCUSSIONS

3.1. The preparation of precursors

After the mechanical milling for 24 h, all the as-milled powders had amorphous similar structures. In the following, we showed as-milled Al_2O_3/FeO_xH_y sample as the typical example to illustrate the effects of mechanical milling on the phase compositions and morphologies of the sample.

Fig. 1(a) showed the XRD spectra of as-milled Al_2O_3/ FeO_xH_y sample. The disappearance of any diffraction peaks indicated amorphous similar structures of the as-milled samples. The phase changes before and after the mechanical milling were well revealed by the results of Mossbauer analysis as shown in Fig. 2 and Table 1. It was obvious that mechanical milling had induced apparent changes in the chemical shift and quadrupole splitting in comparison to those of samples before milling. This meant that the atomic environment of iron species was changed after mechanical milling for 24 h.

Further thermal treatments were conducted for Al_2O_3/- FeO_xH_y samples in order to characterize the detailed effects of mechanical milling on phase changes of the powder. As seen from Fig. 1, the crystallization of as-milled Al_2O_3/ FeO_xH_y samples began at 400 ℃ and the well crystallization was accomplished at 800 ℃.

After calcination, Mossbauer analysis showed that both the chemical shift and quadrupole splitting parameters further decreased with increase of calcination temperatures.

We found that the characteristic doublet due to Fe^{3+} in the samples calcined at 800 ℃ or above was different from that in samples calcined at lower temperature. For the samples calcined at 800 and 1200 ℃, the quadrupole splitting parameters were similar to each other, apparently smaller than those of the samples calcined at lower temperature. For these two samples, the quadrupole splitting parameters were in good agreement with those reported, accounting for the substitutional Fe^{3+} ions in the Al_2O_3 lattice [16–18].

Of noteworthy is the sample calcined at 800 ℃. Only a strong doublet was detected for this sample as shown by the Mossbauer analysis in Fig. 2. This indicated that 20 wt% Fe_2O_3 was fully dissolved into Al_2O_3, apparently higher than the conventional solubility limits (around 15 wt%) of α-Fe_2O_3 in Al_2O_3 phase [18]. XRD analysis (Fig. 1(c)) suggested that as-formed solid solution was monophased that was denoted as $Al_{1.75}Fe_{0.25}O_3$ phase. While for the samples without mechanical milling, such kind of monophased well-crystallized solid solution could not be formed at 800 ℃. It is well known that mechanical alloying can always induce the formation of supersaturated solid solutions, the non-equilibrium phase with composition far from the equilibrium [19–21]. Therefore, the enhanced solubility of α-Fe_2O_3 in α-Al_2O_3 should be ascribed to the activation effects presented by the mechanical alloying.

The as-formed $Al_{1.75}Fe_{0.25}O_3$ solid-solution was a metastable phase. When the sample was calcined at 1200 ℃, the segregation of α -Fe_2O_3 phase took place as shown by Fig. 1(d) and Table 1. Whereas, for the sample with 5 wt% Fe_2O_3, the calcination at both 800 and 1200 ℃ led to the formation of well-crystallized monophased solid solution that was

denoted as $Al_{1.95}Fe_{0.05}O_3$. No segregation of α -Fe_2O_3 phase were observed. This could be readily ascribed to the low content of Fe_2O_3.

Above experimental results suggested that high-energy mechanical milling could induce alloying effects and accelerate the substitution reactions between parent oxides. In Al–Ni–O and Al–Co–O systems, similar experimental results were also found for such alloying effects.

3.2. The reduction of the oxides

As mentioned above, one of the advantages of mechanical milling process over the chemistry-based processes lies in the fact that no thermal treatments are required. Therefore, the nanocrystalline structures obtained after mechanical milling can be maintained before the hydrogen reduction. This will definitely present positive effects on the reduction behaviors of as-milled samples. In the following, we showed as-milled Al_2O_3/NiO_xH_y samples as the typical example.

The reduction behaviors of the Al_2O_3/NiO_xH_y samples at different temperatures were indicated by the results of room-temperature magnetic measurements. The ratios of the as-measured saturation magnetization (M_s) to the theoretic M_s of the samples were taken as the reduction ratios that were plotted versus reduction temperatures as shown in Fig. 3.

As indicated by Fig. 3, it was obvious that the mechanically-milled Al_2O_3/NiO_xH_y samples possessed higher reducibility when compared with co-precipitation derived samples. The co-precipitation derived Al_2O_3/NiO sample underwent the thermal treatment at 500 ℃. The different reducibility between the mechanically-alloyed samples and co-precipitation derived samples could be ascribed to the difference in their morphologies. SEM study (Fig. 4) showed that, after the reduction at 700 ℃, the co-precipitation derived Al2O3/Ni nanocomposites showed much larger particle size of several tens of micrometers. Also the smooth surface as-observed under SEM suggested the possible occurrence of sintering. While for mechanical-milling derived samples, after reduction at 700 ℃, the nanocomposites appeared fine-grained structure with much smaller average particle size. Close analysis of the agglomerates in this sample revealed their rather loose and porous structures. This might be due to the fact that the co-precipitation derived samples underwent the thermal treatment at 500 ℃ before H_2 reduction while no pre-calcination treatment was conducted for the as-milled samples. In this sense, it was reasonable to attribute the high reducibility of mechanically-alloyed samples to their porous and fine-grained structural features. During hydrogen reduction, the porous structure of the as-milled samples provides favorable paths for H_2 penetration, resulting in a greatly accelerated reduction progress.

In addition, from the X-ray analysis, we calculated the Ni particle size for different catalytic powders by using the Scherrer formula. It was found out that average size of as-reduced Ni nanoparticles was around 10 nm.

For the as-milled $Al_2O_3/C_oO_xH_y$ samples, similar results were obtained as indicated by Fig. 2. As to the as-milled Al_2O_3/FeO_xH_y samples, lower reducibility was observed in

comparison to as-milled α-Al_2O_3/NiO_xH_y and α-Al_2O_3/ CoO_xH_y samples. This should be attributed to the low reducibility of iron oxides in terms of thermodynamics. However, when compared with co-precipitation derived Al_2O_3/Fe_2O_3 sample, the mechanical-milling derived sample still possessed apparent higher reducibility.

3.3. The growth of CNTs

Above experimental results indicated that mechanical milling could be an efficient way to produce oxide/metal nanocomposites. The high reducibility of the as-milled samples and the nanometric size of as-reduced metal nanoparticles suggest the promising potential of mechanical milling in the production of suitable catalytic nanocomposites for the growth of CNTs. In the following, we demonstrated that the mechanical-milling derived catalysts could be ideal candidates for the catalytic growth of either multi-walled or SWCNTs.

3.3.1. The effects of the preparation processes of catalyst precursors

In order to compare the catalytic behaviors of the catalysts prepared by different processes, two kinds of processes, mechanical alloying and co-precipitation were employed to produce the Al_2O_3/Ni catalyst powders in this work. The catalysts reduced at 450 ℃ were used for the catalytic growth of CNTs. The comparison between the CNTs derived from these two different catalysts indicates much higher efficiency of CNT growth on the mechanical alloying-derived catalyst. As shown by Fig. 5, the yield of CNTs was apparently higher for mechanical alloying-derived catalyst (Fig. 5(b)) than that for the co-precipitation-derived catalyst (Fig. 5(a)). As shown in Fig. 5(a), the Al_2O_3 matrix particles were so less covered by CNTs that their primary surfaces and edges could be clearly observed. While in Fig. 5(b), the thick web of CNTs made the particles appear as downy spheres. The higher yields for the for mechanical alloying-derived catalysts can be readily attributed to the higher content of Ni phase after reduction, as indicated by Fig. 2, although both catalysts and CNT products were obtained under the same conditions. Fig. 6(a) and (b) were the TEM images of CNTs grown the co-precipitation derived catalysts and mechanical alloying-derived catalysts. For both cases, the obtained CNTs appeared as long and curved multi-walled tubes. The diameters of these tubes were uniform throughout the length and in the range of 10–15 nm.

3.3.2. The effects of different kinds of catalysts

For mechanical alloying derived Al_2O_3/Co catalysts, their catalytic behaviors for the growth of MWCNTs were similar to those of Al_2O_3/Ni catalysts. Fig. 7(a) showed the SEM image of CNTs grown on Al_2O_3/Co catalysts with the same growth conditions as those for Al_2O_3/Ni catalysts. Bountiful CNTs were obtained that densely covered the surface of the matrix grains, indicating the high activity of Al_2O_3/Co catalysts for the growth of CNTs. TEM analysis showed that CNTs obtained from Al_2O_3/Co catalysts were also multi-walled and these tubes were generally long with uniform diameters through the length, as seen from Fig. 8(a).

For mechanical alloying derived Al_2O_3/Fe catalysts, their growth conditions of CNTs were quite different those of Al_2O_3/Ni and Al_2O_3/Co catalysts. Due to the low reduction ratio of Fe_2O_3 phase, there was no apparent carbon deposition for Al_2O_3/Fe catalysts at the temperatures below 600 ℃. Therefore, in the following we showed the CNTs grown on Al_2O_3/Fe nanocomposites at the temperature of 1000 ℃ by using one-step method.

Fig. 7(b) showed the SEM image of CNTs grown at 1000 ℃ in H_2/CH_4 mixture gases by using mechanical milling-derived Al_2O_3/Fe nanocomposites. As seen from them, the as-obtained carbon products appeared as somewhat and short and curved filaments. Beside these short filaments, a lot of spherical particles were also observed under SEM. TEM analysis showed that these filaments were thick-walled CNTs, as seen from Fig. 8(b). Therefore, different from Al_2O_3/Ni and Al_2O_3/Co catalysts, the mechanical alloying derived Al_2O_3/Fe catalyst showed much low catalytic activity for the growth of multiwalled CNTs. However, things were different when the $Al_{1.75}Fe_{0.25}O_3$ solid solution was used as the catalyst precursors. As seen from Fig. 7(c), many long and straight filaments were observed. TEM analysis revealed that these long and straight filaments were CNT bundles that consisted of small tubes (Fig. 8(c)). These were typical SWCNTs under low-magnification TEM. Besides these SWCNTs, some amounts of short, curved tubes and spherical nanoparticles were observed. Therefore, the comparison between Fig. 7(b) and (c) or Fig. 8(b) and (c) clearly indicated that the calcination of Al_2O_3/Fe_2O_3 samples at 800 ℃ was helpful for improving the catalytic activity for the CNTs growth. This might be related to the more uniform distribution of Fe species in the alumina matrix due to the formation of solid solution phase. The in situ formed Fe nanoparticles from solution matrix were very small and uniformly dispersed and thus active enough for the formation of SWCNTs. This was further verified by the CNTs grown on $Al_{1.95}Fe_{0.05}O_3$ solid solution derived catalysts. As shown by Fig. 7(d), CNTs grown on these catalysts were usually straight and long with the length up to several tens of micrometers. They were tangled and cross linked together and formed thick webs that fully covered the surface of the matrix grains, suggesting the high productivity of CNTs. Fig. 8(d) was the typical TEM images of CNTs as shown in Fig. 7(d). Under low-magnification TEM, the straight CNTs observed under SEM were found to be CNTs bundles, same as those in Fig. 7(c). These bundles were cross-intersected together. Some bundles were as large as several tens of nanometers in diameters. High-resolution TEM analysis revealed that these CNT bundles consisted of SWCNTs with the diameters around 3–5 nm. Under high-resolution TEM, we selected 100 nanotubes for the rough estimation of the productivity of SWCNTs. It was found out that over 95% of CNTs were single-walled.

Therefore, by using the mechanical alloying-derived $Al_{1.95}Fe_{0.05}O_3$ precursors, we realized the large-scale production of SWCNTs. Such kind of high productivity of SWCNTs embodied the advantages of mechanical alloying-derived catalyst precursors for the growth of CNTs. On the one hand, mechanical alloying can accelerate the substitutional reactions between parent oxides and thus realize the low-temperature formation of well-crystallized solid solution. As a result, the fine-grained and porous structure of precursors were formed that made less catalyst precursors be trapped inside matrix grains. Therefore, upon reduction, more active catalytic sites were available for the formation of SWCNTs. In this sense, mechanical alloying process makes low catalyst

loading feasible and favorable for producing SWCNTs with high yields. The low catalyst loading and the nature of the simple processing setting-up of mechanical alloying might provide a convenient and cost-efficient way for large-scale production of SWCNTs.

4. CONCLUSION

Mechanical alloying was employed to produce Al_2O_3/ transition metal (Fe, Co, Ni) nanocomposites on which large-scale formation of MWCNTs and SWCNTs were achieved. It was found out that:

1. The mechanical milling could result in the drastic refinement and uniform dispersion of catalyst precursors;
2. Compared with co-precipitation-derived catalyst precursors, mechanical-milling derived Al_2O_3/NiO precursors possessed porous and fine-grained structure. This resulted in their high reducibility and the high yield of MWCNTs;
3. Mechanical milling can induce solid-state alloying and accelerate the substitutional reactions between parent oxides (Al_2O_3 and Fe_2O_3). This led to the formation of monophased well-crystallized $Al_xFe_yO_z$ solid solution after low-temperature thermal treatment;
4. The fine-grained and porous structures of low-temperature formed $Al_xFe_yO_z$ solid solutions made the low¬catalyst-loading feasible and favorable for the large-scale production of single-walled carbon nanotubes (SWCNTs). Over 95% of carbon nanotubes were SWCNTs when using equilibrium $Al_{1.95}Fe_{0.05}O_3$ solid solutions as the catalyst precursors.

REFERENCES

[1] Lau KT, Hui D. The revolutionary creation of new advanced materials: carbon nanotube composites. Compos Part B: Engng 2002;33:263.
[2] Pelgney A, Laurent Ch, Rousset A. J Mater Chem 1999;9:1167.
[3] Zhong Z, Chen H, Tang S, Ding J, Lin J, Lee KT. Chem Phys Lett 2000;330:41.
[4] Liu BH, Zhong ZY, Ding J, Lin JY, Shi Y, Si L. J Mater Chem 2001; 11:2523.
[5] Hafner JH, Bronikowski MJ, Azamian BR, Nikolaew P, RInzler AG, Colbert DT, Smith KA, Smalley RE. Chem Phys Lett 1998;196:185.
[6] Flahaut E, Govindaraj A, Peigney A, Rousset A, Rao CNR. Chem Phys Lett 1999;300:236.
[7] Koch CC. Nanostruct Mater 1993;2:109.
[8] Schwarz RB, Koch CC. Appl Phys Lett 1986;49:146.
[9] Ding J, Miao WM, McCormick PG, Street R. Appl Phys Lett 1995;67: 3804.
[10] Ding J, McCormick PG, Street R. J Magn Magn Mater 1997;171:309.
[11] Cabrera AF, Sanchez FH. Phys Rev B 2002;65:094202.
[12] Zhou ZH, Xue JM, Wang J, Chan HS, Yu T, Shen ZX. J Appl Phys 2002;91:6015.
[13] Cui XL, Wang L, Qi M. J Mater Sci Technol 2001;17:S89.
[14] Ding J, McCormick PG, Street R. J Magn Magn Mater 1997;171:309.
[15] Ding J, McCormick PG, Street R. Phys Status Solidi B 1999;172:469.
[16] Peigney A, Laurent Ch, Dumortier O, Rousset A. J Eur Ceram Soc 1998;18:1995.
[17] Verelst M, Kannan KR, Subbanna GN, Rao CNR. J Mater Res 1992; 11:3072.
[18] Laurent Ch, Peigney a, Rousset A. J Mater Chem 1998;8:1263.
[19] Zhou ZH, Xue JM, Wang J, Chan HSO, Yu T, Shen ZX. J Appl Phys 2002;91:6015.
[20] Gupta A, Dhuri P. Mater Sci Engng A 2001;304:394.
[21] Abdellaoui M, Gaffet E, Barradi T, Faudot F. IEEE Trans Magn 1994; 30:4887.

List of Figures

List of Table

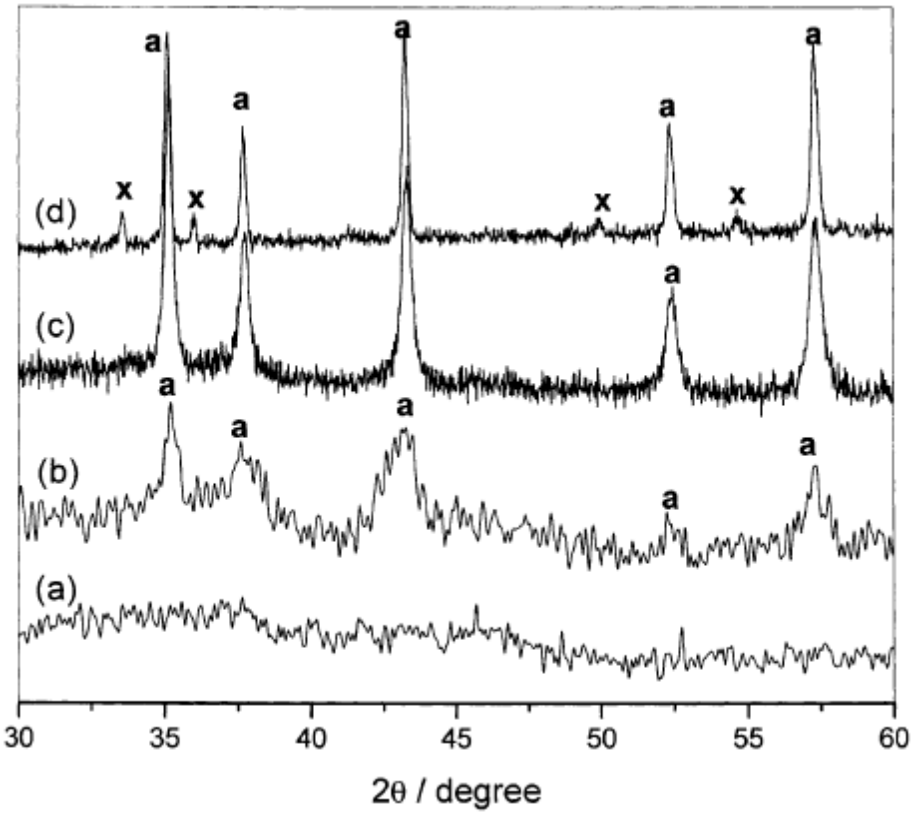

Figure 1

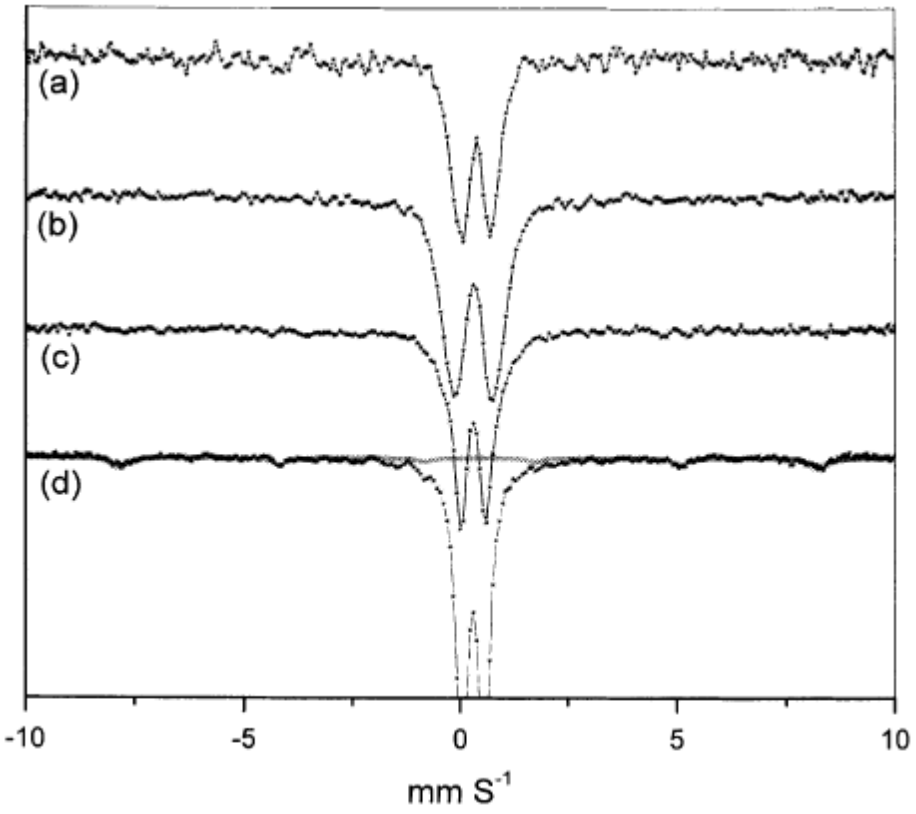

Figure 2

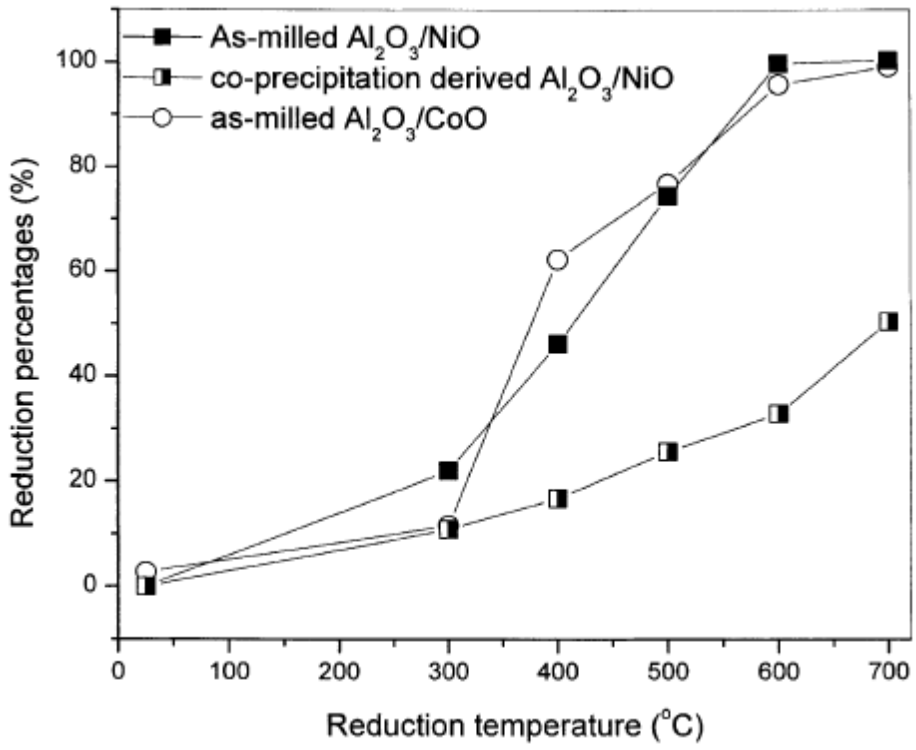
As-milled Al_2O_3/NiO
co-precipitation derived Al_2O_3/NiO
as-milled Al_2O_3/CoO
Reduction percentages (%)
Reduction temperature (°C)
0
20
40
60
80
100
0
100
200
300
400
500
600
700

Figure 3

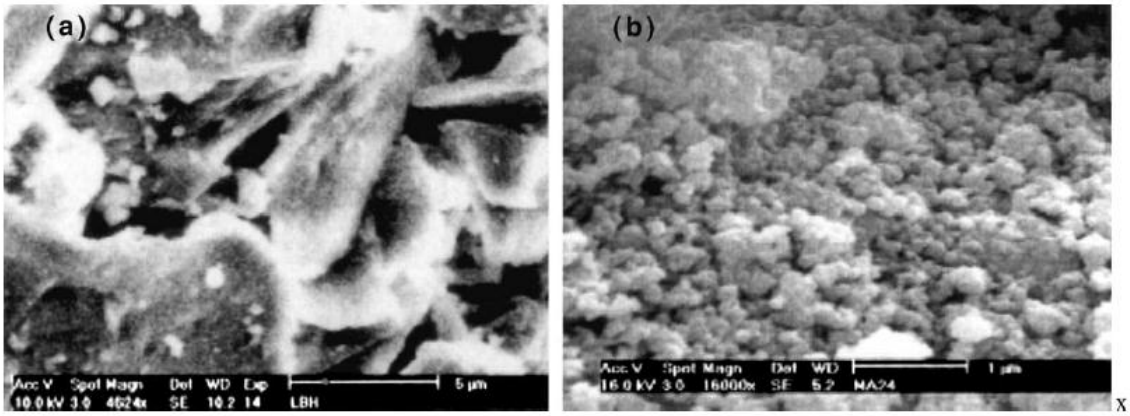
(a)
Acc.V Spot Magn Det WD Exp
10.0 kV 3.0 4624x SE 10.2 14 LBH
5 µm
(b)
Acc.V Spot Magn Det WD
16.0 kV 3.0 16000x SE 5.2 MA24
1 µm

Figure 4

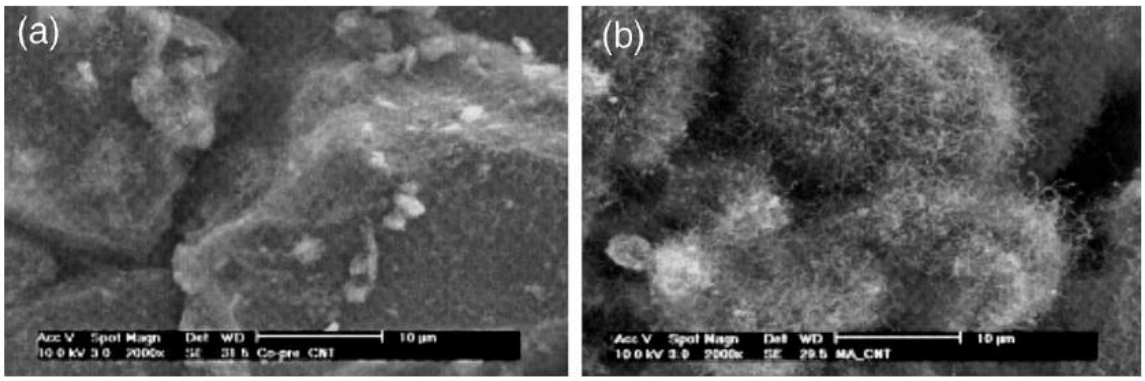

Figure 5

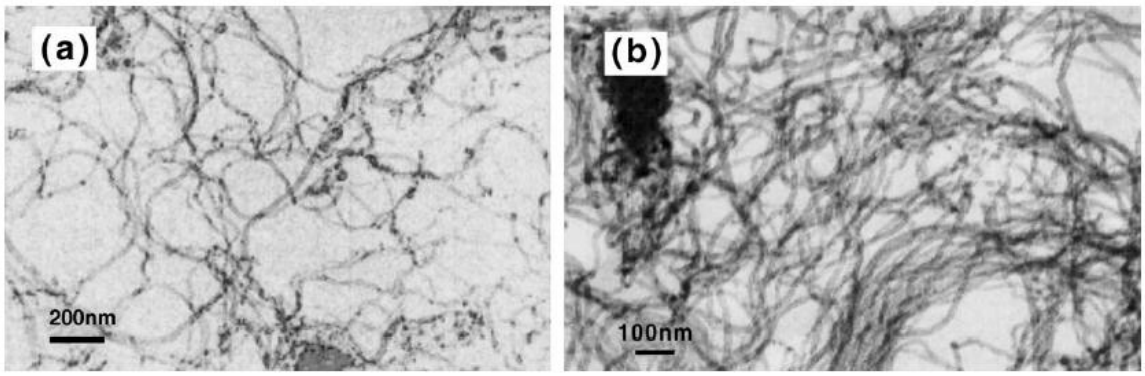

Figure 6

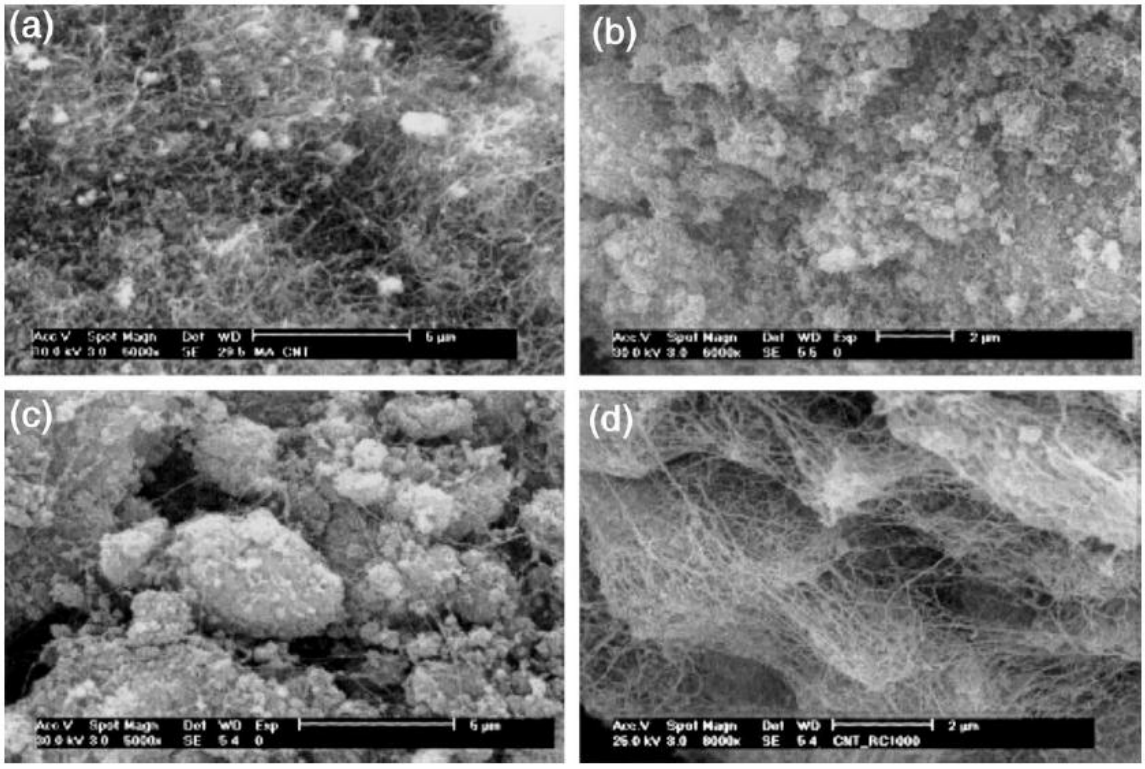

Figure 7

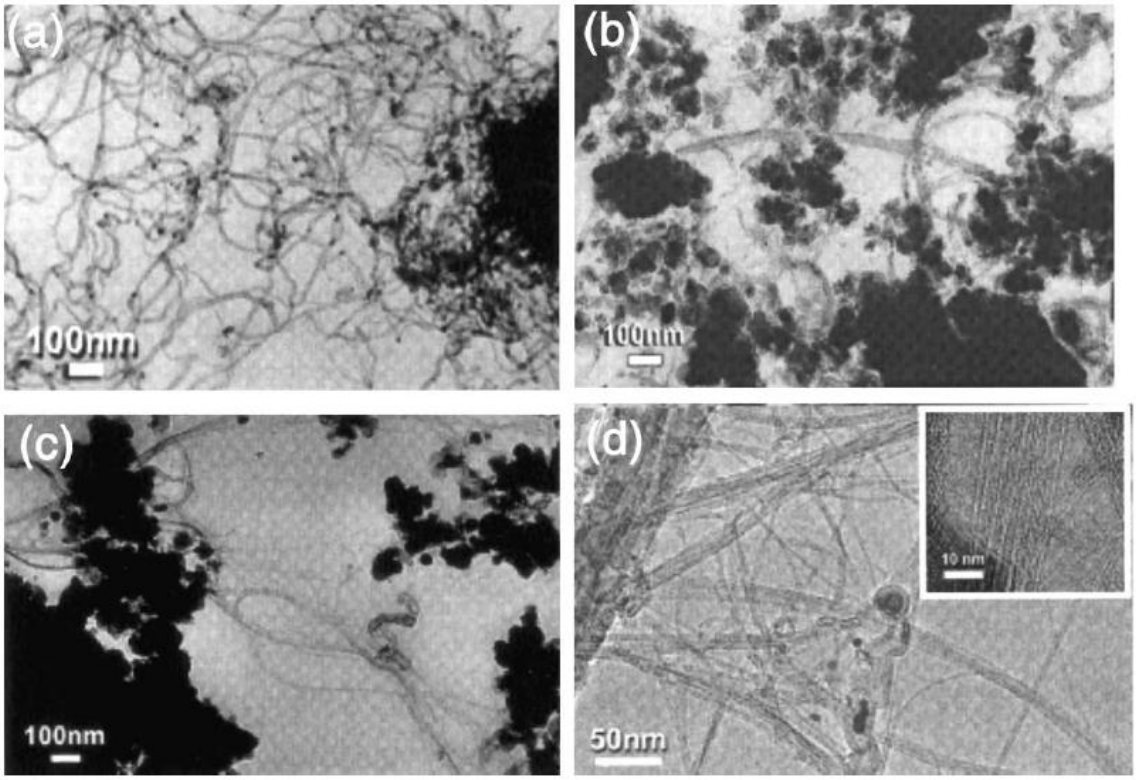

Figure 8

Sample	Doublet			Sextet		
	CS (mm s^{-1})	ΔE_Q (mm s^{-1})	P (%)	CS (mm s^{-1})	H (T)	P (%)
Powder without milling	0.355	0.717	100	–	–	–
MA24 (as-milled for 24 h)	0.312	0.938	100	–	–	–
MA24/A400 °C	0.308	0.912	100	–	–	–
MA24/A800 °C	0.303	0.599	100	–	–	–
MA24/A 1200 °C	0.298	0.572	91.34	0.334	49.745	8.66

Table 1